Eng. Sci., 2022, **17,** 274–284

Engineered Science

DOI: https://dx.doi.org/10.30919/es8d557

Enhancing the Axial Ratio Bandwidth of Circularly Polarized Open Ground Slot Coplanar Waveguide-Fed Antenna for Multiband Wireless Communications

Sandeep Kumar Singh,[1, 2,*] Tripurari Sharan[2] and Arvind Kumar Singh[2]

Abstract

This article presents a new structure of a coplanar waveguide (CPW) antenna to enhance its performance by using optimal electrical dimensions. A circularly polarized (CP) broadband open-ground slot antenna has been proposed and analyzed in this work. It resembles a cross-shaped CPW feed structure that is placed in the middle of the square slot antenna. The overall size of the antenna is $0.66\lambda_c \times 0.66\lambda_c \times 0.01\lambda_c$ at 4 GHz (where λ_c represents the wavelength corresponding to the center frequency (f_c) of the 3-dB CP bandwidth). The antenna is fabricated on the same plane of a flame-retardant fiberglass epoxy (FR4) microwave dielectric substrate. Broadband CP operation is achieved by embedding two-square ring slits on the ground plane. Also, to obtain wider impedance bandwidth (IBW) and axial-ratio bandwidth (ARBW), a cross-shaped tuning stub feed line strip and an open slot in the ground plane are used. The peak gain of the proposed antenna is about 5.7 dBi at 3.5 GHz. The results are compared with the reported works. The proposed structure provides a larger ARBW with the same dielectric substrate and comparable size.

Keywords: Multiband; WLAN; WiMAX; IMT; open-slot antenna; ARBW; CPW.
Received: 24 June 2021; Revised: 22 October 2021; Accepted: 23 October 2021.
Article type: Research article.

1. Introduction

The wireless communication technology for audio and video transmission and reception is developing at an extremely fast rate, which demands well-sophisticated, compact, and high-performance trans-receiver types of equipment. To pace with the demand and supply of these devices, it becomes necessary to upgrade them from generation to generation. The newly invented and upgraded products must also be available in the market at the same rate. Both the transmitter and receiver sections of the communication system need to be highly efficient broadband antennas.[1,2] The demand for the compact receiving antenna, for portable handheld equipment, is growing gradually. The portable communication system requires a very compact, radiation efficient, and printed CPW antenna with broadband CP operations.[3] A planar geometry triple-band CP antenna is designed for wireless applications such as worldwide interoperability for microwave access (WiMAX), wireless local area network (WLAN), industrial, scientific, and medical (ISM) radio band, international mobile telecommunication (IMT), Bluetooth, and wireless fidelity (Wi-Fi). The antenna consists of rectangular strips on the upper surface along with rectangular slots on the ground plane.[4] A broadband CP square-slot antenna based on an inverted L-shaped microstrip feed line is proposed for C-band applications.[5] The design of smart and high-performance CP antenna for wireless communication systems has become an essential need of the day due to its enhanced service quality and capability of larger ARBW.[6]

A monopole antenna is proposed using FR4 dielectric substrate and two open-ground planes for CP operations. Both the bandwidth of ARBW and IBW is enhanced by loaded dual stubs and dual parasitic strips on the ground plane.[7] A miniaturized CP ultrawide-band antenna loaded by an annular-ring slot is presented for application in different wireless communication devices. The structure shows improvements in the operating frequency band and comprehension of the CP radiation.[8] The other attractive features of CP antennae are namely-adverse weather condition tolerance and non-requirement of alignment to achieve an accurate polarization between antennas.[9] The CP antenna excites two orthogonal

[1] *Department of EECE, SET, Sharda University, Greater Noida, India.*

[2] *North Eastern Regional Institute of Science and Technology, Nirjuli, Arunachal Pradesh, India.*

**E-mail*: sandeepsingh.ec@sharda.ac.in (S. Singh)

modes of radiation pattern acting in the phase quadrature. This distinctiveness afforded by such antennas has made them gradually more popular for wireless applications.[10] Antenna designers in general choose different shapes of the slots such as square, rectangular, and ring with appropriate tuning stubs and substrate materials.[11-13]

A low-profile compact spiral antenna with a broad-band CP response is proposed. Among such antennas, spiral antennas have received a momentous amount of attention over the past several decades due to their ultra-wideband characteristics, radiation patterns over the whole frequency band of operation, and practically compact and low-profile dimensions.[12] Various techniques have been proposed by different groups to increase the ARBW of antennas. The geometrical design configuration of the ground and radiating plane of a slot antenna has been modified in different ways to increase the ARBW.[14] Large dimensions and limited IBW characteristics are the main limitations of CP antennas. However, the configuration and geometrical designs of the CP antenna have very complex provisions and fabrication processes as well.[15,16] A high-gain wideband CP antenna might have different types of symmetric or asymmetric structures with various shapes of the radiating patch.[17] The proposed antenna consists of four triangular radiation patches and a compact feed network. Each of the radiation patches is grounded by shorting pins for 3-dB ARBW enhancement and patch miniaturization.[18] A novel technique is used for the enhancement of the bandwidths by mode merging of the CP dielectric resonator antenna.[19] The wideband performance of the antenna is ensured by using different shapes of tuning stubs and modified ground plane structure, as reported.[20,21]

In this paper, a circularly polarized open-slot configured CPW-fed antenna has been proposed. From the literature survey, it was very much evident that the existing antenna structures were having one or more than one of the following disadvantages: (1) They were not able to provide multiband input impedance matching. (2) They were not able to provide good radiation patterns, gain, voltage standing wave ratio (VSWR), and ARBW. The novelty of this work is that it mitigates the above-listed limitations.

The proposed structure of the antenna is simulated on finite integration technique (FIT) in computer simulation technology (CST) version 17 (V.17) electromagnetic (EM) simulator in the antenna template transient mode. The results of the proposed CPW antenna such as return loss, VSWR, ARBW, and gain have been achieved and shown good agreement between measured and simulated results in CST. The optimal frequency range from 1.5 to 6.0 GHz is carried out using a FIT-based CST EM simulator. The design and evaluation steps of the antennas are described in the following sections. The proposed antenna configurations with utilized design methodologies are explained in section 2, and section 3 covers the optimization with a parametric study of the proposed antenna. Section 4 analyzes its performances, and comprehensive comparison with other reported works, and finally, section 5 concludes with the future scope of this research.

2. Antenna geometry and evolution

Some asymmetric prototypes of antennas have been developed and investigated very recently as illustrated in Fig.1. Four differing antenna configurations are being reported and compared in this paper. The first one, as denoted by antenna-1, contains simple straight-line feeding, Fig. 1(a); the second one recognized as antenna-2 uses a wider stub at the top side of the feeding line, Fig. 1(b); the third one described as antenna-3 has a cross-shaped CPW-fed tuning stub as illustrated in Fig. 1(c). The fourth one, the proposed antenna named antenna-4, presents the structure, which contains a cross-shaped microstrip CPW feeding line with two asymmetric square rings located at the substrate plane as shown in Fig. 2(a). This structure provides significantly enhanced CP-bandwidth and IBW as compared to the antenna structures reported.[9] The antenna-4 uses additional asymmetrical square-shaped rings in the lower left and right side of the ground plane, which has ensured a wider impedance bandwidth and ARBW as well.

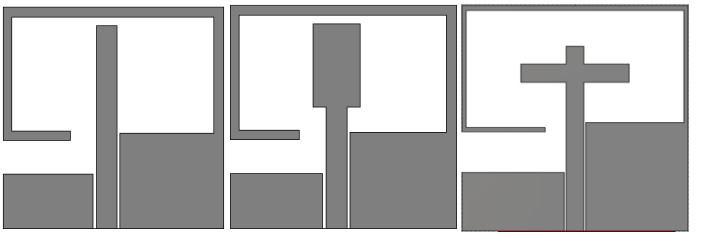

Fig. 1 Evolution steps of the CP open-slot CPW antennas: (a) Antenna 1: Design process of basic structure with a wide straight (I-shaped) feeding line, (b) Antenna 2: It is designed using a wider stub at the top side of I shaped feeding line and (c) Antenna 3: It is designed using a cross-shaped tuning stub feeding line.

Figure 2(a) shows the geometry of this circularly polarized proposed antenna, whose conductor is printed on a square-shaped FR4 substrate of a thickness (h), 0.8 mm, relative permittivity (ε_r) of 4.4, and dielectric loss tangent (tan δ) of 0.02. The area of the substrate plane (L×W) is chosen to be 50×50 mm^2. Fig. 2(b) shows the fabricated die-photograph of antenna-4. The excitation signal is fed through a 50 Ω CPW feeder line to this antenna. It has a cross-shaped tuning stub of a width of 4 mm and a width gap between ground planes of 0.35 mm from the center of the ground plane towards the Y-axis direction (see Fig. 2(a)). The proposed antenna-4 has square slit rings towards both the left and right sides which are etched on the ground plane of the substrate. The thickness of square rings is 1mm, and side lengths are 10 mm and 6 mm from the right and left arms, respectively.

2.1 Antenna geometry optimization

The structure modeling of the antenna is the most important

class for the design of the particular antenna. Different kinds of materials and geometries are used for modeling the structure of the antenna. The geometries are used for enhancing the antenna parameters namely return loss, bandwidth, gain, and radiation pattern of the antenna. Mathematical modeling has been introduced in this paper for determining the dimensions of the antenna and the applied optimization techniques to improve the antenna performance. The designed antenna is useful for wideband purposes only possible through a suitable selection of antenna size, where the antenna dimension can be minimized.

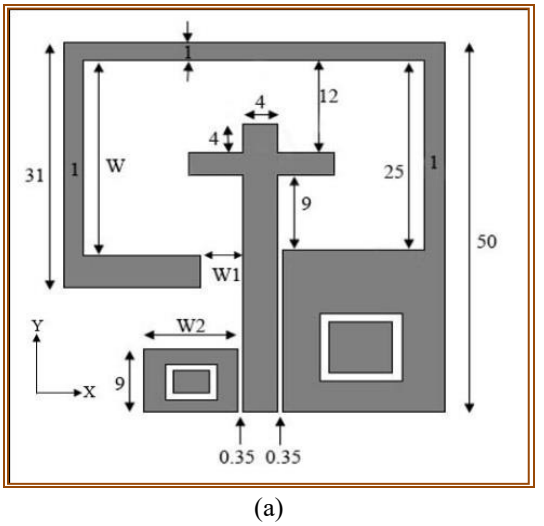

(a)

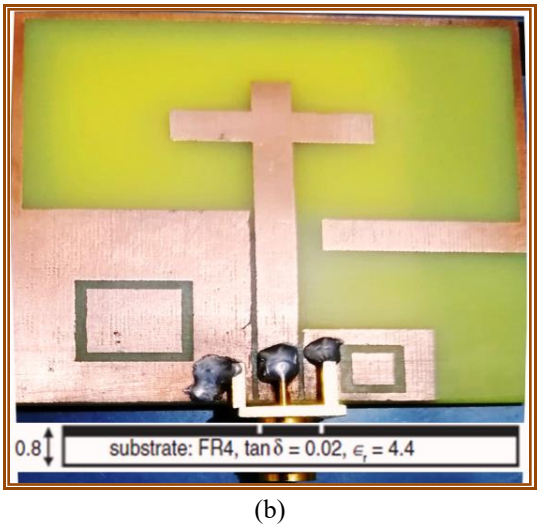

(b)

Fig. 2 Schematic configuration of broadband CP open-slot antenna fed by CPW: (a) front view of a proposed antenna-4, and (b) die-photograph of the fabricated antenna-4 with a bottom view.

The resonant frequency (f_r), radiation pattern, and input impedance are now controlled by the length (L) and width (W) of the patch. If the W is large, it can raise the bandwidth range. The following formulae compose further development for basic calculations of the antenna dimensions. The L and W of the patch antenna can be calculated by using Equations (1-5).[21]

2.1.1 Calculation of the width (W)

$$W = \frac{1}{2fr\sqrt{\mu 0\varepsilon 0}}\sqrt{\frac{2}{1+\varepsilon r}} \quad (1)$$

$$W = \frac{c}{2fr}\sqrt{\frac{2}{1+\varepsilon r}} \quad (2)$$

where $c = \frac{1}{\sqrt{\mu 0\varepsilon 0}}$ is the velocity of light in the free space, μ_0 is the permeability of free space, ε_0 is the permittivity of free space, ε_r is the relative permittivity of the substrate, and f_r is the resonant frequency.

2.1.2 Actual length of the patch (L)

$$L = L_{eff} - 2\Delta L \quad (3)$$

$$L = \frac{1}{2fr\sqrt{\mu 0\varepsilon 0}\sqrt{\varepsilon reff}} - 2\Delta L \quad (4)$$

$$L = \frac{c}{2fr\sqrt{\varepsilon reff}} - 2\Delta L \quad (5)$$

where ΔL is the incremental length due to the Fringing field, and ε_{reff} is the relative effective dielectric constant. The effective dielectric constant can be calculated by using Equation (6), and the effective length (L_{eff}) can be calculated using Equation (7).

$$\varepsilon r_{eff} = \frac{\varepsilon_r+1}{2} + \frac{\varepsilon_r-1}{2}\left(\frac{1}{\sqrt{1+\frac{12h}{w}}}\right) \quad (6)$$

$$Leff = \frac{c}{2fr\sqrt{\varepsilon reff}} \quad (7)$$

The open-slot CPW-fed antenna has been configured in the X and Y plane. The ground plane has been opened in the X-direction and strip line feeding (CPW) has been designed in the Y-direction. The magnetic current distribution in the XY-plane produces two orthogonal modes with the same amplitude but out of phase (± 90°, phase quadrature) with each other. This is called circularly polarized EM radiation, which confirmed a good ARBW. The schematic configuration of the proposed antenna-4 is illustrated in Figs. 2(a) and (b), have been fairly improved as compared to antenna structures depicted in Figs. 1(a & b), whose geometry is reported.[9] Antenna design steps are illustrated in Table 1 along with geometrical parameters as well as electrical specifications of the antennas. The geometrical parameters W, W_1, and W_2 about the open slot for this structure have been detailed in section 3.

2.2 Antenna performance with various feeding

In this section, the performance of the proposed antenna-4 has been examined and compared with the antennas of different CPW-feed lines having various shapes as reported.[9] Fig. 3 shows simulated performances of antennas-4, antenna-1, antenna-2, and antenna-3 to compare their characteristics. The simulated VSWR and ARWB results of these four antennas are shown and summarized in Figs. 3(a & b), and Table 1. The impedance bandwidths of all antennas are identified by the operating frequency range with VSWR ≤ 2. The CPW-feed broadband circularly polarized square slot antennas referred to as antenna-1 and antenna-2 (illustrated in Fig. 1) have a similar

shape to reference antenna-1 and antenna-2,[9] but their dimension is a bit different which improves their ARBW. The axial ratio (AR) bandwidth (AR≤ 3 dB) of modified antennas 1 and 2 is found to be 32% and 30%, which are 8.9% and 3% more than the values found for the concerned reference antennas reported.[9]

The total IBW of antenna-3 is 91.12% (1.80–3.25 GHz, and 5.15–6.90 GHz) and ARBW 23% (0.90 GHz, 3.45–4.35 GHz). Owing to the use of a cross-shaped feed line, the antenna-3 ensured the dual-band (IBW) characteristics of 1.45 GHz (60.4%) and 1.75 GHz (30.7%), respectively as illustrated in Fig. 7(a). It confirmed the first resonant frequency (f_{r1}) of 2.5 GHz at -25 dB return loss and the second resonant frequency (f_{r2}) of 5.8 GHz at -50 dB return loss. The resonant frequency ratio (f_{r2}/f_{r1}) of antenna-3 is found to be 2.38 (see Table 1), which is less than the central frequency of Wi-MAX (f_c = 2.5 GHz) and WLAN (f_c = 5.8 GHz) bands and thus makes it suitable for dual-band applications. The antenna-3 is expected to be useful in dual-band applications in linear-polarization characteristics for Wi-MAX (2.50–2.69 GHz), and WLAN (5.725–5.825 MHz) bands. The antenna-3 can also be used for ISM and Bluetooth (f_c = 2.4 GHz, 2.40–2.48 GHz).

The proposed antenna-4 has a broad IBW of 85.71% (3.6 GHz, 2.4–6.0 GHz) and also ensures VSWR ≤ 2 for the entire frequency range. It can be used in a linear polarization operation for the IMT band (f_c = 2.8 GHz, 2.7–2.9 GHz), high-performance microwave links, U4 band, (f_c = 4.4 GHz, 4.46–4.52 GHz), and WLAN band, (f_c = 5.2 GHz, 5.15–5.35 GHz), respectively as illustrated in Fig. 7(b). Its CP band covers a frequency range from 2.62 to 5.42 GHz (ARBW = 2.8 GHz, 70%) with AR ≤ 3 for the entire CP frequency range. Moreover, antenna-4 has a cross-shaped microstrip feed line with two asymmetric square rings located at its substrate plane, which ensures the largest CP bandwidth among other antennas as depicted in Table 1.

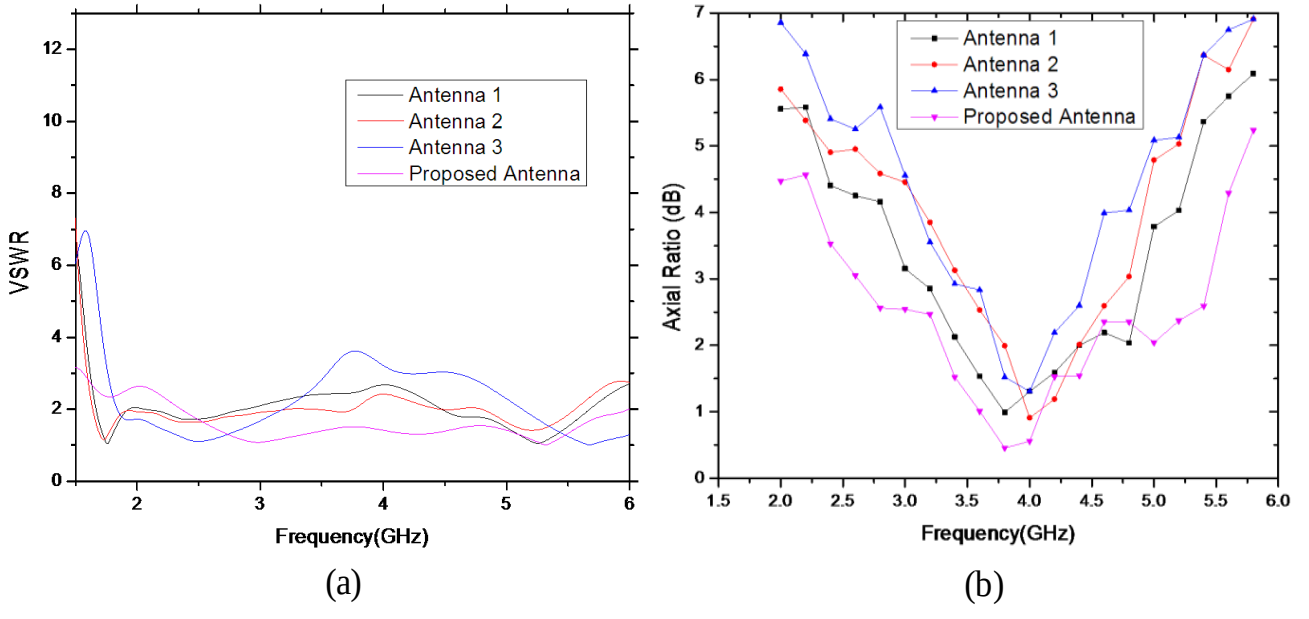

(a) (b)

Fig. 3 Comparison of evaluated and proposed antenna-4 performance parameters: (a) VSWR and (b) ARBW.

Table 1. Design parameters and performances of all antennas to develop proposed antenna-4.

Antenna Evolution Steps	Geometrical Design Specifications			Electrical Specifications of Antenna							
	W (mm)	W_1 (mm)	W_2 (mm)	f_{r1} (GHz)	IBW_1 (-10 dB) (GHz, %)	f_{r2} (GHz)	IBW_2 (-10 dB) (GHz, %)	f_{r3} (GHz)	IBW_3 (-10 dB) (GHz, %)	f_{r2}/f_{r1}	ARBW (3-dB) (GHz, %)
Antenna 1	19	3.0	22.65	1.75	1.15, 65.7	5.25	0.87, 16.6	NA	NA	3.00	1.20, 32
Antenna 2	20	3.5	22.65	1.60	1.36, 85.0	5.20	0.90, 17.3	NA	NA	3.25	1.25, 30
Antenna 3	21	4.0	22.65	2.40	1.45, 60.4	5.70	1.75, 30.7	NA	NA	2.38	0.90, 23
Antenna 4 (Proposed)	22	2.5	12.65	2.80	1.40 (-12dB), 50.0	4.40	0.80 (-16 dB), 18.2	5.20	0.50 (-16 dB), 9.6	1.85	2.80, 70

NA: not applicable, f_{r1}: resonant notch frequency-1, f_{r2}: resonant notch frequency-2, f_{r3}: resonant notch frequency-3, f_{r2}/f_{r1}: resonant frequency ratio.

3. Parametric study of antenna-4

The impedance matching of antenna-4 as illustrated in Fig. 2(a), the geometrical design parameters of the asymmetric ground plane W, W1, and W2 about the open slot are carried out by using an EM simulator (CST V.17). To investigate the influence of these geometrical design parameters (W, W1, and W2) on IBW and ARBW characteristics of the concerned antenna, one geometrical design parameter is changed at a time, while keeping the remaining two parameters fixed. The length of ground slots is widely used to achieve the notch bands in the wideband CPW antennas. Depending on the user's requirements, these notch bands can easily be controlled by changing the length of slots.[21] The length of these open ground slots (W, W1, and W2) can be found in the notch frequencies by using Equation (8).

$$fNotch = \frac{c}{2LGroundSlot\sqrt{\varepsilon reff}} \quad (8)$$

where f_{Notch} is the fundamental resonating frequencies of the open ground slot, and $L_{Ground\ Slot}$ is the length of the ground slots. The results of these parametric simulations are shown in the following subsections.

3.1 Variation effect of parameter "W"

In Fig. 2(a), the length of left-arm ground (W) is varied from 18 to 26 mm to ensure an enhanced CP bandwidth. The geometrical parameter W affects the electrical parameters of the CP antenna when the relative position of this open ground slot in the Y-direction is varied. Fig. 4 illustrates the effect of changing the parameter W while keeping W1 = 4.0 mm, and W2 = 22.65 mm, on the CP behavior of the antenna, although the placement of the slot (W) at the right position is the biggest challenge for the designer.[21] Thus, a judicious analysis was carried out to identify the correct position of the slot (W = 22 mm) by approximating from Equation (9).

$$fNotch = \frac{c}{2LW\sqrt{\varepsilon reff}} \quad (9)$$

where LW is the length of the open ground slot (W).

The simulated |S11| for wide-band is depicted in Fig. 4(a). Figs. 4(a & b) depicts that the well-optimized results for IBW (2.4 – 6.0 GHz, S11 ≤ –10 dB) and ARBW (2.62 – 5.42 GHz, AR ≤ 3 dB) are obtained when W ranges from 21 to 23 mm. Thus, the cross-tuning stub with a modified ground of the antenna-4 having W = 22 mm, W1 = 4.0 mm and W2 = 22.65 mm (see Fig. 2(a)) can be considered as a suitable selection for a broadband CP antenna.

3.2 Variation effect of parameter "W1"

The effect of the gap distance (W1) between the cross-shaped tuning stub and the open ground slot in the x-direction upon the return loss and axial ratio bandwidth is examined in this part. The gap width W1 is varied from 2.5 to 6.5 mm while keeping W = 22 mm and W2 = 22.65 mm, the return loss and axial ratio of antenna-4 are simulated, and the results are shown in Figs. 5(a & b). Fig. 5(b) illustrates all the results (CP axial ratio) of antenna-4, which depicts that the best favorable value of AR has approached 0.5 dB which is a much less critical requirement of 3 dB. The best position of the open ground slot (W1 = 2.5 mm) can be approximated by using Equation (10).

$$fNotch = \frac{c}{2LW1\sqrt{\varepsilon reff}} \quad (10)$$

where LW1 is the length of the open ground slot (W1). It is achieved for W1 = 2.5 mm, W = 22 mm, and W2 = 22.65 mm, It has been found that the parameter (W1) is responding to the changes in the axial ratio behavior. The best value of achieved AR is about 0.5 dB.

3.3 Variation effects of parameter "W2"

In Fig. 2(a), the length of left ground (W2) is varied from 12.65 to 22.65 mm while keeping W = 22 mm, and W1 = 2.5 mm as constant. The suitable position of the open ground slot (W2 = 12.65 mm) can be approximated using Equation (11).

$$fNotch = \frac{c}{2LW2\sqrt{\varepsilon reff}} \quad (11)$$

where LW2 is the length of the open ground slot (W2).

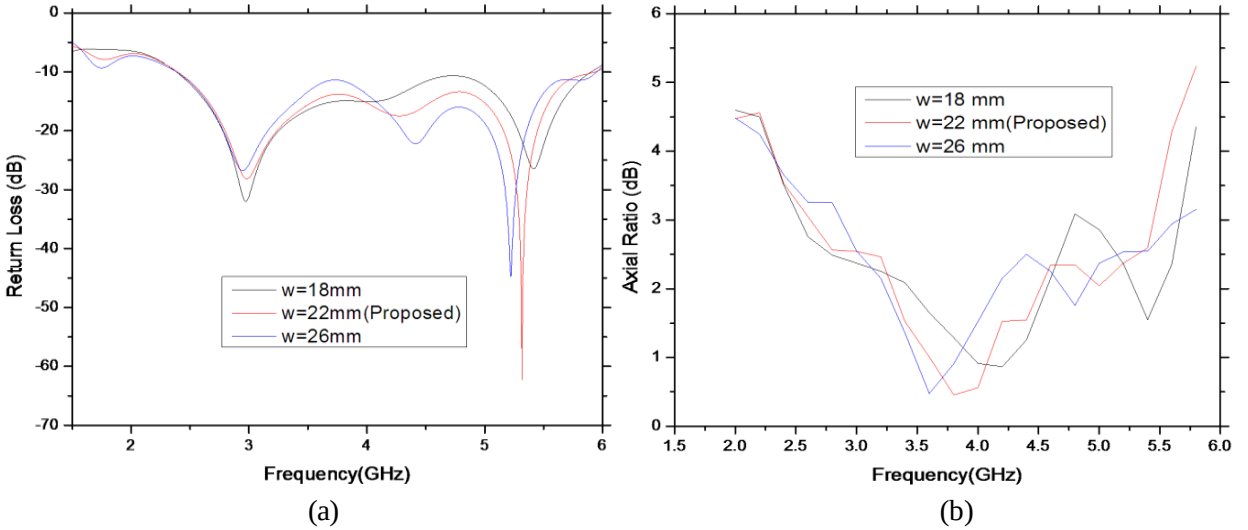

(a) (b)

Fig. 4 Effects of W variation (18 mm ≤ W ≤ 26 mm) on antenna performance: (a) Return loss and (b) ARBW.

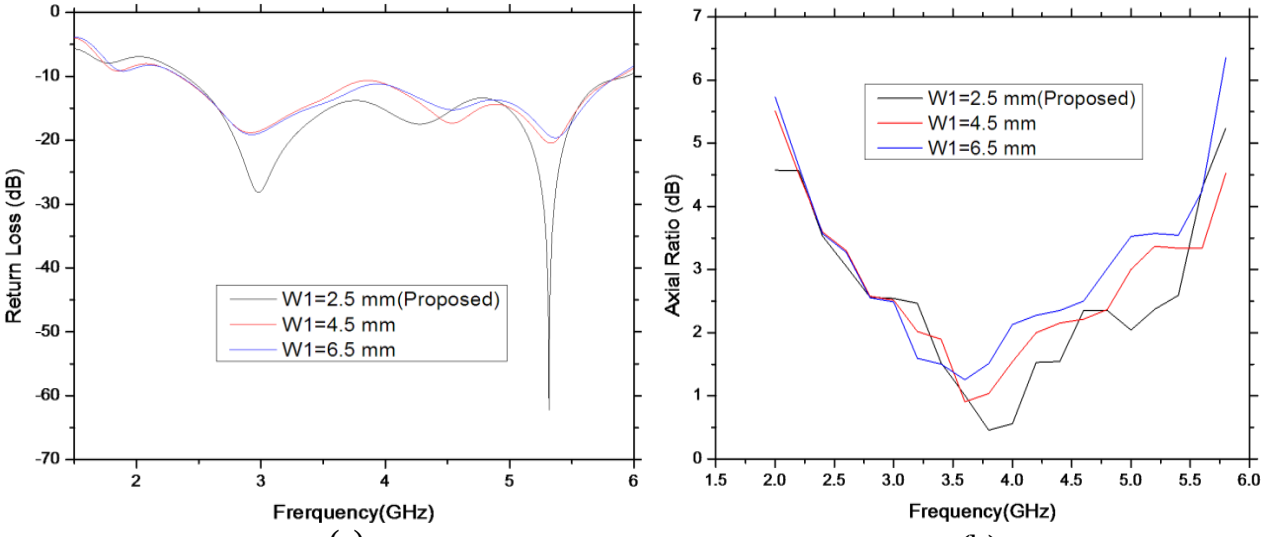

Fig. 5 Effects of W_1 variation (2.5 mm ≤ W_1 ≤ 6.5 mm) on antenna performance: (a) Return loss and (b) ARBW.

Figures 6(a & b) illustrates the results of return loss (IBW = 3.6 GHz, 85.71%) and CP axial ratio (ARBW = 2.8 GHz, 70%) of the proposed antenna-4. The best favorable result concerned with CP broadband applications is obtained for W2 = 12.65 mm, W = 22 mm, and W1 = 2.5 mm. The lengths of an asymmetric ground plane W, W1, and W2 have been most effective for best impedance bandwidth and axial-ratio bandwidth. Based on this parametric study, the optimized ground parameters of suggested antenna-4 are listed in Table 1. Thus, the best results have been found for ground plane dimensions of W = 22 mm, W1 = 2.5 mm, and W2 = 12.65 mm (see Fig. 2(a)). These optimized ground plane dimensions have ensured broadband CP characteristics.

4. Results and discussion

The performances and results of antenna-4 have been simulated and measured using an EM simulator (CST V.17) and a vector network analyzer. Different parametric investigations of this antenna are necessary for any CP-broadband antenna and are carried out. The proposed design, largely enhanced ARWB at the 3-dB, is about 70% (2.8 GHz, 2.62–5.42 GHz, relative to the center frequency of 4 GHz) to cover from 2.7–2.9 GHz (f_c = 2.8 GHz) for IMT band-1, from 3.40–3.69 GHz (f_c = 3.5 GHz) for WiMAX band, from 4.4–4.9 GHz (f_c = 4.6 GHz) for IMT band-2, and from 5.15–5.35 GHz (f_c = 5.2 GHz) for WLAN band, respectively as illustrated in Fig. 3(b). Fig. 7(a) shows the simulated return losses of all four antennas whereas Fig. 7(b) shows the simulated and measured results (return loss, S_{11} ≤ –10 dB) of antenna-4. The simulated and measured results are found in good agreement.

To examine the feed-line vector surface current distribution for different time phases at ωt = 0°, ωt = 90°, ωt = 180°, and ωt = 270°, related to the proposed circularly polarized antenna,

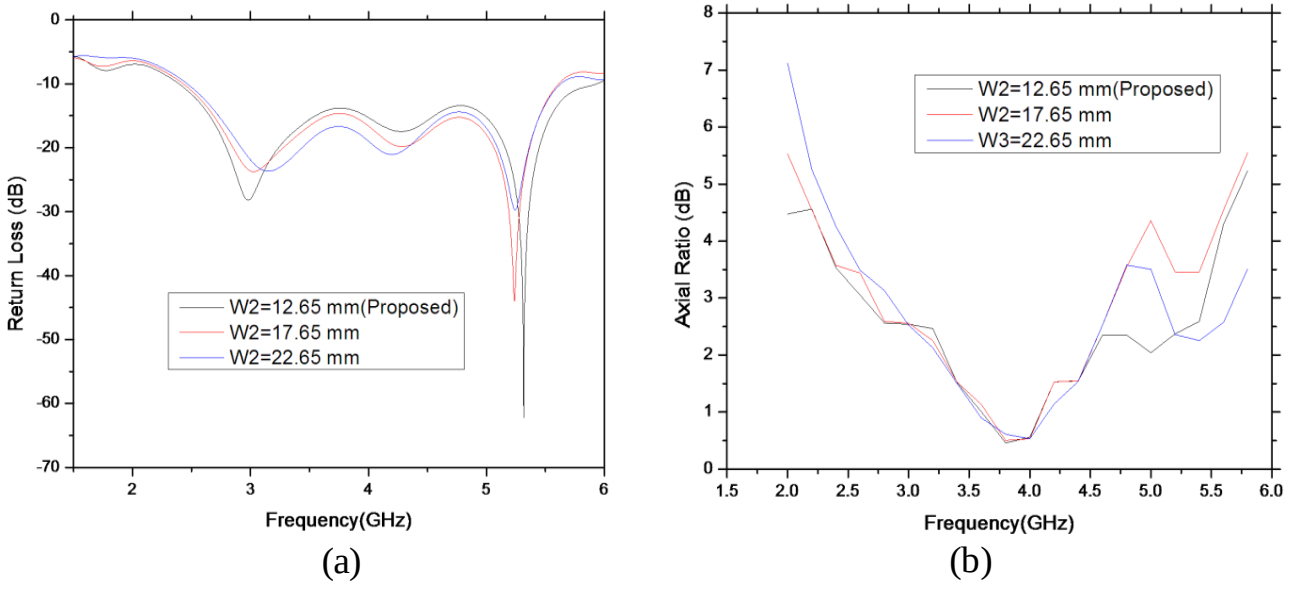

Fig. 6 Effects of W_2 variation (12.65 mm ≤ W_2 ≤ 22.65 mm) on performance: (a) return loss and (b) ARBW.

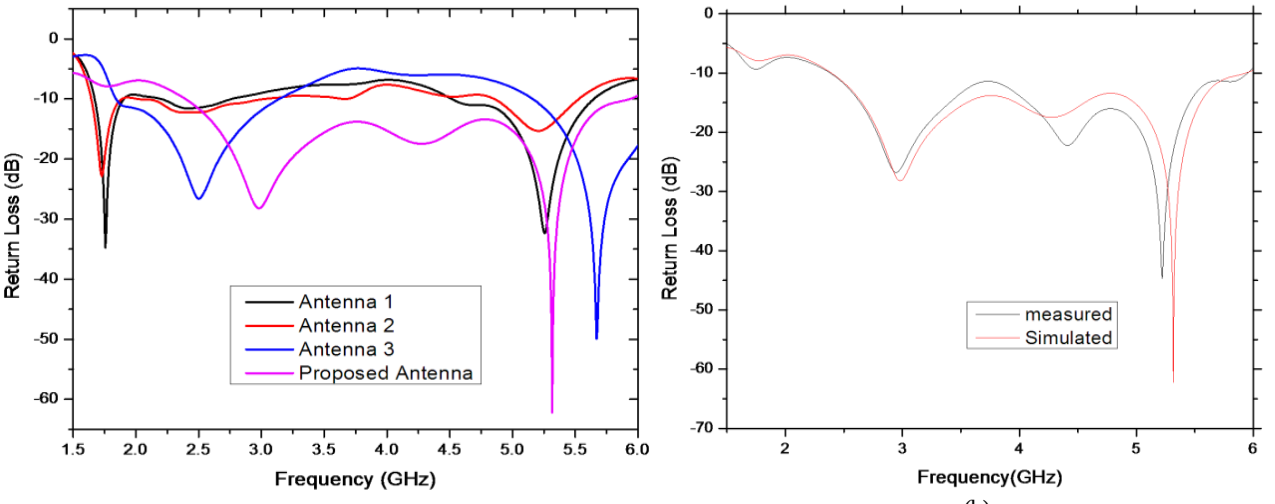

Fig. 7 Return loss: (a) simulated results of all four antennas and (b) measured result of the proposed antenna-4.

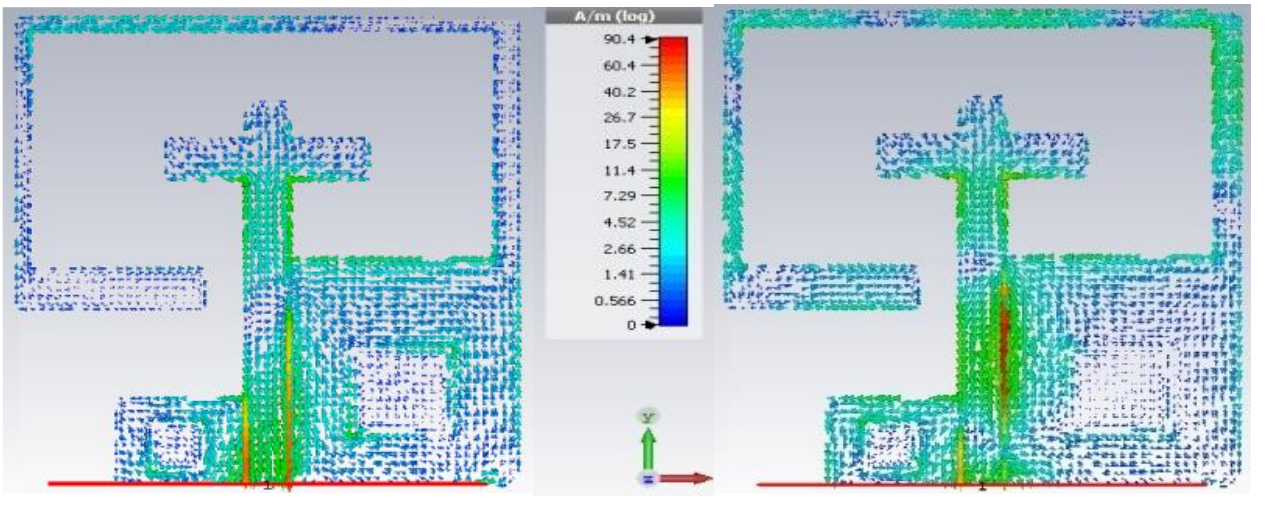

Fig. 8 Simulated vector surface current distribution of antenna-4 at Centre frequency 4GHz, from 2.62 to 5.42GHz: (a) Surface current density at ωt = 0° (180°) and (b) Surface current density at ωt = 90° (270°).

the simulations are performed. Figs. 8(a & b) shows the vector surface current distributions of antenna-4 at center frequency 4 GHz plotted at ωt = 0° (180°) as well as at ωt = 90° (270°). Fig. 8(b) presents the magnetic surface current distribution, which is just 90° phase inversion to that of Fig. 8(a). The magnetic surface current distribution is varying as a function of time in such a fashion that the phase reversal of the current vector occurs for 0° and 180°, and 90° and 270° as well. At 4 GHz, the main current directions for time phases 0° and 90° are shown in the +X and +Y directions. Instead, the current directions for time phase 180° and 270° are aligned in the −X and –Y directions having the same amplitude but opposite in phases of 0° and 90°, respectively. As a result, the surface current vector passes along in a clockwise direction in the XY-plane, therefore the proposed antenna radiates as a circularly polarized wave in space.

The radiation pattern of an antenna is a graphical representation of the radiation properties of the antenna. Graphically, we surround the antenna with a sphere and evaluate
the electric and magnetic fields (far-field radiation fields) at a distance equal to the radius of the sphere. Figs. 9 and 10 show the simulated and measured far-field radiation patterns of antenna-4 at Phi = 0° and Phi = 90° in the XY and YZ-planes at the center frequency 4 GHz. The measured radiation patterns have matched in a pleasant way with simulated radiation patterns. The radiation patterns have lower A values around the broadside directions which are suitable and satisfactory for the CP antenna.

The gain of the antenna is equal to the directivity of the antenna times its efficiency. The gain represents the focusing power ability of the antenna including its losses. Despite mentioning the directivity of the antenna, very often its maximum gain is quoted. Fig. 11 shows that the peak gain of antenna-4 is approximately 5.7 dBi at 3.5GHz. The achieved antenna gain has an average value of 4.5 dBi with a variation

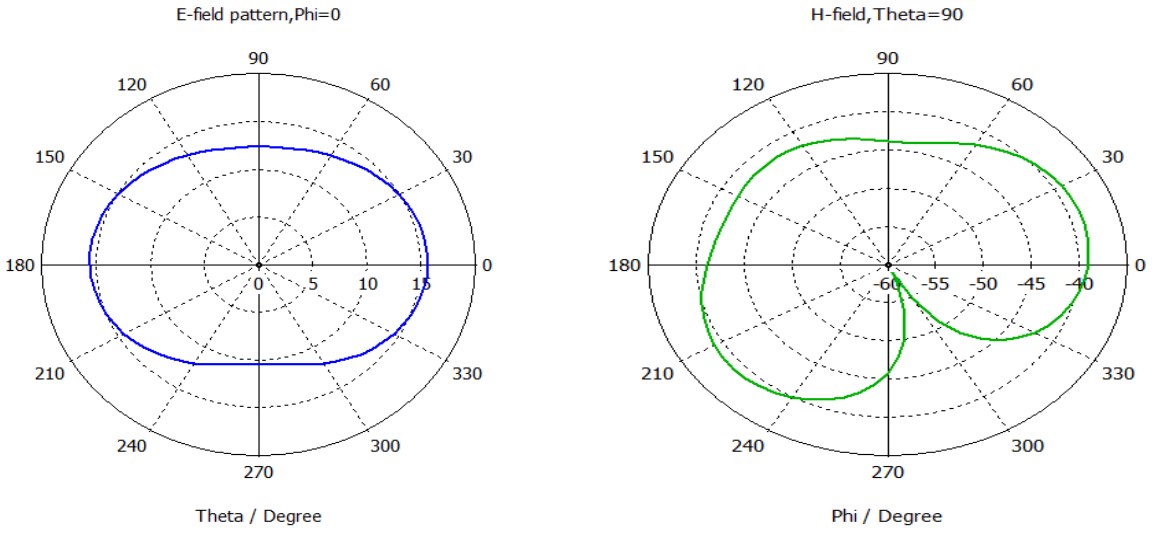

Fig. 9 Simulated radiation patterns of the antenna-4 at 4 GHz: (a) E-plane, and (b) H-plane.

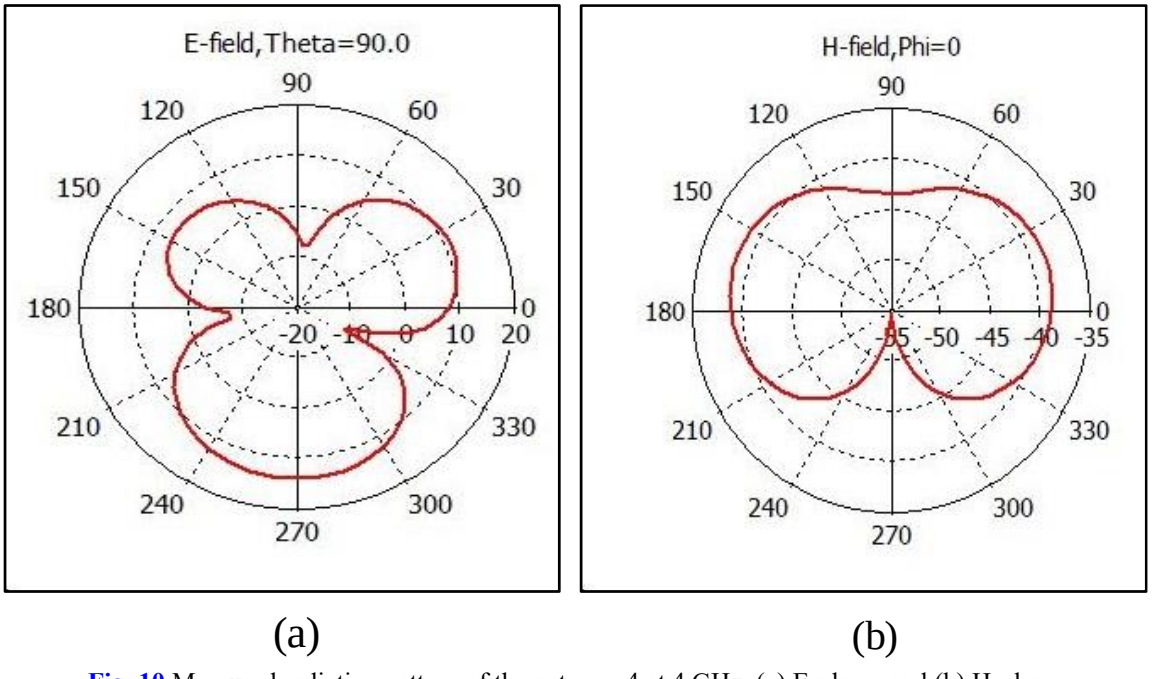

Fig. 10 Measured radiation pattern of the antenna-4 at 4 GHz: (a) E-plane, and (b) H-plane.

of ±1 dBi over the 3-dB ARBW.

Table 2 lists the overall performances of antenna-4 and some other referred works [1–3, 6, 9-11, 13, and 15–20] for comparison purposes. Table 2 is arranged to compare the performances of proposed antenna-4 with the previously reported antennas [1–3, 6, 9-11, 13, and 15–20], that is also fabricated on the same dielectric substrate (FR4, $\varepsilon_r = 4.4$, $\tan\delta = 0.02$) for a fair comparison. Although the overall area of proposed antenna-4 is identical to the reported antenna,[9] its ARBW (70%) is larger among all the works mentioned in Table 2.

After carrying out an extensive literature survey of the available antenna structures and comparing their performance with the proposed antenna it can be concluded that the proposed structure offers the following advantageous features over the existing structures: (1) In terms of ARBW, the proposed structure is having an ARBW almost equal to 70% with 2.8 GHz (compared with [3], [6], [13], [16], [19] and [20]) which have respectively 31%, 50%, 64%, 46%, 54% and 57% with 0.68 GHz, 1.5 GHz, 2.1 GHz, 1.3 GHz, 3.2 GHz, and 1.38 GHz respectively. (2) In terms of IBW, the proposed structure is performing far better than the existing structures

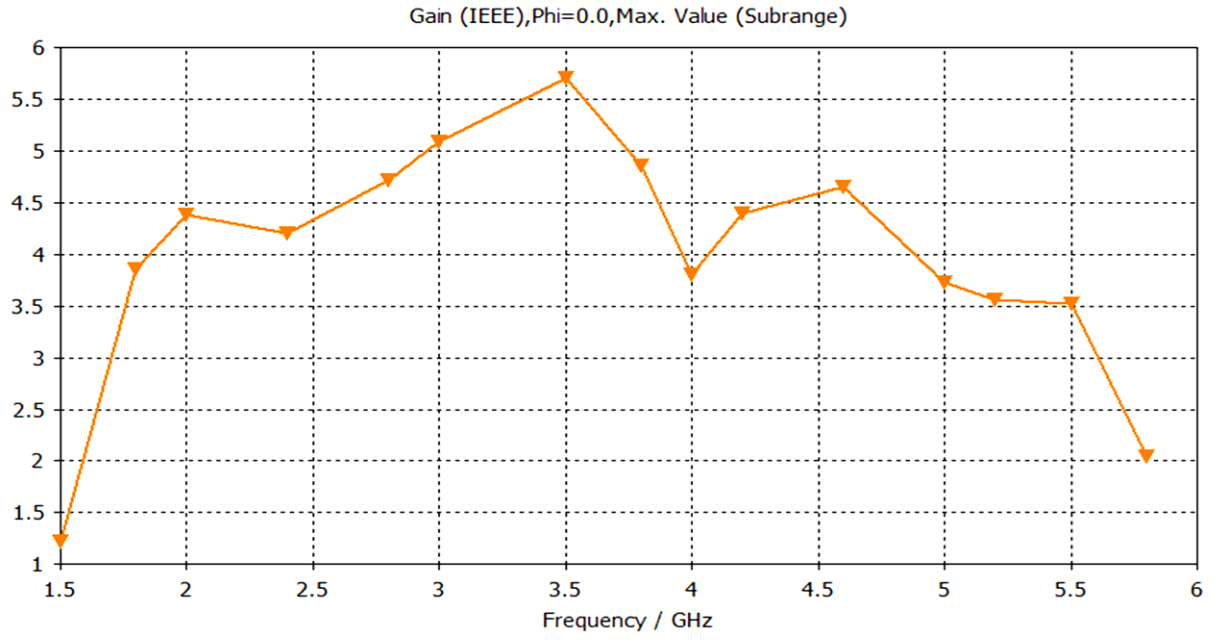

Fig. 11 Gain of proposed antenna-4 across the entire CP operating frequency range.

Table 2. Comparison of the antenna-4 with other published reported works.

References	$f_{c\,(ARBW)}$ (GHz)	IBW ($S_{11}\leq$ -10dB) (GHz, %)	ARBW (AR ≤ 3 dB) (GHz, %)	Peak Gain (dBi/dBic)	Antenna Area $(\lambda_c)^2$	Reported (Years)
[1]	2.0	- -	0.36, 18	4.0	0.47 × 0.47	2003
[2]	1.9	0.85, 40	0.24, 12	3.5	0.46 ×0.46	2007
[3]	2.2	0.82, 35	0.68, 31	4.1	0.44 × 0.44	2008
[6]	3.0	2.70, 86	1.50, 50	4.3	0.62 ×0.62	2011
[9]	3.7	5.33, 111	1.00, 27	5.3	0.62 × 0.62	2013
[10]	5.5	8.50, 118	1.22, 22	3.5	0.46 × 0.46	2014
[11]	2.7	2.33, 75	1.30, 47	3.7	0.46 × 0.37	2014
[13]	3.0	2.00, 63	2.10, 64	2.0	0.39 × 0.39	2016
[15]	6.1	3.35, 56	2.60, 43	2.3	0.45 × 0.33	2018
[16]	2.8	3.28, 111	1.30, 46	3.5	0.71 × 0.60	2019
[17]	5.9	4.80, 72	2.03, 34	8.6	0.98 × 0.98	2020
[18]	0.9	0.17, 18	0.35, 39	5.1	0.41 × 0.41	2021
[19]	5.9	4.36, 68	3.20, 54	1.2	1.59 × 1.59	2021
[20]	2.4	1.78, 68	1.38, 57	5.4	0.85 × 0.85	2021
This work	4.0	3.60, 85.71	2.80, 70	4.5	0.66 × 0.66	-

except for the structures proposed in [9], [10] and [16]. But since the main objective of this paper is to enhance the ARBW, so the proposed structure serves the purpose, for which it is designed.

5. Conclusion

In the present exposition, the design procedure of novel broadband circularly polarized CPW-fed open slot antenna has been demonstrated. The open ground slot with a modified cross-fed line ensures good CP operation. Moreover, the use of a cross-fed tuning stub and two square-ring slits in the ground plane have extremely enhanced the 3-dB AR bandwidth to 70 % (2.8 GHz, 2.62–5.42 GHz) and antenna gain to around 4.5 dBic which are suitable for IMT, WiMAX,

and WLAN bands. In this work, different configurations of CPW antennas have been successfully designed and implemented in CST. Based on the parametric study, the proposed antenna is quite simple, easy to fabricate, and suitable to design the broadband trans-receive system. Thus, it can be deployed in multiband wireless communications.

Conflict of interest

There are no conflicts to declare.

Supporting information

Not applicable.

References

[1] J. Y. Sze, K. L. Wong, C. C. Huang, Coplanar waveguide-fed square slot antenna for broadband circularly polarized radiation, *IEEE Transactions on Antennas and Propagation*, 2003, **51**, 2141-2144, doi: 10.1109/tap.2003.815421.

[2] C. C. Chou, K. H. Lin, H. L. Su, Broadband circularly polarised cross-patch-loaded square slot antenna, *Electronics Letters*, 2007, **43**, 485, doi: 10.1049/el: 20070189.

[3] J.-Y. Sze, J.-C. Wang, C.-C. Chang, Axial-ratio bandwidth enhancement of asymmetric-CPW-fed circularly-polarised square slot antenna, *Electronics Letters*, 2008, **44**, 1048, doi: 10.1049/el: 20081858.

[4] I. Fatima, A. Ahmad, S. Ali, M. Ali, M. Iram Baig, Triple-band circular polarized antenna for wlan/Wi-Fi/bluetooth/wimax applications, *Progress in Electromagnetics Research C*, 2021, **109**, 65-75, doi: 10.2528/pierc20121207.

[5] M. Midya, A. Ghosh, M. Mitra, Meander-line-loaded circularly polarized square-slot antenna with inverted-L-shaped feed line for C-band applications, *IET Microwaves, Antennas & Propagation*, 2021, **15**, 1425-1431, doi: 10.1049/mia2.12125.

[6] S.-W. Zhou, P.-H. Li, Y. Wang, W.-H. Feng, Z.-Q. Liu, A CPW-fed broadband circularly polarized regular-hexagonal slot antenna with L-shape monopole, *IEEE Antennas and Wireless Propagation Letters*, 2011, 10, 1182-1185, doi: 10.1109/lawp.2011.2172570.

[7] K. Mondal, Axial Ratio (AR) and Impedance Bandwidth (IBW) enhancement of Circular Polarized (CP) monopole antenna, *AEU - International Journal of Electronics and Communications*, 2021, **134**, 1–15, doi: 10.1016/j.aeue.2021.153649.

[8] Z. H. Ma, J. X. Chen, P. Chen, Y. F. Jiang, Design of planar microstrip ultrawideband circularly polarized antenna loaded by annular-ring slot, *International Journal of Antennas and Propagation*, 2021, **2021**, 1-10, doi: 10.1155/2021/6638096.

[9] J. Y. Jan, C. Y. Pan, K. Y. Chiu, H. M. Chen, Broadband CPW-fed circularly-polarized slot antenna with an open slot, *IEEE Transactions on Antennas and Propagation*, 2013, **61**, 1418-1422, doi: 10.1109/tap.2012.2231926.

[10] H. Shirzad, M. Shokri, Z. Amiri, S. Asiaban, B. Virdee, Wideband circularly polarized square slot antenna with an annular patch, *Microwave and Optical Technology Letters*, 2014, **56**, 229-233, doi: 10.1002/mop.28016.

[11] Nasimuddin, X. Qing, Z. N. Chen, Dual-square-ring-shaped slot antenna for wideband circularly polarized radiation, *Microwave and Optical Technology Letters*, 2014, **56**, 2645-2649, doi: 10.1002/mop.28663.

[12] T.-Y. Shih, N. Behdad, A compact, broadband spiral antenna with unidirectional circularly polarized radiation patterns, *IEEE Transactions on Antennas and Propagation*, 2015, **63**, 2776-2781, doi: 10.1109/tap.2015.2414476.

[13] R. Pazoki, A. Kiaee, P. Naseri, H. Moghadas, H. Oraizi, P. Mousavi, Circularly polarized monopole L-shaped slot antenna with enhanced axial-ratio bandwidth, *IEEE Antennas and Wireless Propagation Letters*, 2016, **15**, 1073-1076, doi: 10.1109/lawp.2015.2492918.

[14] M. Nosrati, N. Tavassolian, Miniaturized circularly polarized square slot antenna with enhanced axial-ratio bandwidth using an antipodal Y-strip, *IEEE Antennas and Wireless Propagation Letters*, 2017, **16**, 817-820, doi: 10.1109/lawp.2016.2605099.

[15] K. O. Gyasi, G. Wen, D. Inserra, Y. Huang, J. Li, A. E. Ampoma, H. Zhang, A compact broadband cross-shaped circularly polarized planar monopole antenna with a ground plane extension, *IEEE Antennas and Wireless Propagation Letters*, 2018, **17**, 335-338, doi: 10.1109/lawp.2018.2789430.

[16] S. Das, H. Islam, T. Bose, N. Gupta, Ultra wide band CPW-fed circularly polarized microstrip antenna for wearable applications, *Wireless Personal Communications*, 2019, **108**, 87-106, doi: 10.1007/s11277-019-06389-9.

[17] A. Kumar, S. Dwari, G. P. Pandey, B. K. Kanaujia, D. K. Singh, A high gain wideband circularly polarized microstrip antenna, *International Journal of Microwave and Wireless Technologies*, 2020, **12**, 678-687, doi: 10.1017/s1759078719001612.

[18] Z. Wang, Y.-N. Wang, X. Liu, H. Liu, S.-J. Fang, A compact broadband circularly-polarized patch antenna with wide axial-ratio beamwidth for universal uhf rfid applications, *Progress in Electromagnetics Research C*, 2021, **113**, 1-11, doi: 10.2528/pierc21032704.

[19] A. Kumar, R. S. Yaduvanshi, Design and analysis of circularly polarized dielectric resonator antenna, *Wireless Personal Communications*, 2021, **118**, 2663-2673, doi: 10.1007/s11277-021-08148-1.

[20] W. He, Y. He, S. W. Wong, C. H. Liao, A wideband circularly polarized S‐shaped slot antenna, *International Journal of RF*, 2021, **31**, 1–9, doi: 10.1002/mmce.22612.

[21] J. Acharjee, A. K. Singh, K. Mandal, S. K. Mandal, Defected ground structure toward cross polarization reduction of microstrip patch antenna with improved impedance matching, *Radioengineering*, 2019, **27**, 33-38, doi: 10.13164/re.2019.0033.

Author Informmation

Sandeep Kumar Singh *received his B. Tech degree and M.Tech degree in Electronics & Communication Engineering from the FET RBS College, Agra, India, and HBTI, Kanpur, India, in 2001, and 2004, respectively. He is currently pursuing his Ph.D. from the North Eastern Regional Institute of Science and Technology, Nirjuli, Arunachal Pradesh, India. Since 2005 he is working as an Assistant Professor in the Department of Electronics & Communication Engineering, Sharda University, Greater Noida, India. His research interest includes the RF and microwave integrated circuits.*

Tripurari Sharan *obtained his B. Tech degree in Electronics Engineering from Kamla Nehru Institute of Technology, Sultanpur UP, India in 1989 and M. Tech. degree in VLSI Design from the Department of Electronics and Communication Engineering of North Eastern Regional Institute of Science and Technology (NERIST), Deemed to be University, Nirjuli, Arunachal Pradesh India, in 2010. He obtained his Ph.D. degree under QIP schemes from the ECE department of MNNIT, Prayagraj Allahabad, UP, India in March 2018. He has been working as an Assistant Professor in the ECE Department of NERIST since July 2001. He is a member of IET, IEEE, and a lifetime member of IETE, ISTE professional bodies. He is an active reviewer of AICSP, IEEE Access, BMT, and IETE (Taylor and Francis) Journals. His research activities are focused on the design of Low-voltage, low-power, Linear Analog VLSI, and Mixed Integrated Circuits.*

Arvind Kumar Singh *earned his bachelor's and master's degrees in Electrical Engineering from BIT, Sindri, Dhanbad, India in 1988 and 1991, respectively. He received his Ph.D. degree in Electrical Machine and Drive from Tezpur Central University, Tezpur, Assam, India, in 2006. Dr. Singh is currently Professor for electrical machine and drive, and power systems at the Department of Electrical Engineering, North Eastern Regional Institute of Science and Technology, Nirjuli, Arunachal Pradesh, India. Dr. Singh has authored and co-authored over 42 technical peer-reviewed papers in international journals and conference proceedings. His current research interests include the machine drive and power system, HVDC, and EHV-AC transmission line.*

